Application of MCR-ALS with EFA on FT-IR Spectra of Lipid Bilayers in the Assessment of Phase Transition Temperatures: Potential for Discernment of Coupled Events

Petra Maleš[Δ, a], Zlatko Brkljača[Δ, b], Ivo Crnolatac[b], Danijela Bakarić[b, *]

[a] Division of Analytical Chemistry, Department of Chemistry, Faculty of Science, University of Zagreb, Horvatovac 102a, 10000 Zagreb, Croatia

[b] Division for Organic Chemistry and Biochemistry, Ruđer Bošković Institute, Bijenička 54, 10000 Zagreb, Croatia

[Δ] (P. M., Z. B.) Both authors contributed equally to the manuscript.

Abstract

Elucidation of the origin of the ripple phase displayed by multibilayers constituted from phosphatidylcholine lipids is a rather challenging task from both experimental and computational perspective. Despite apparent supremacy of various structural techniques in characterizing the periodic undulations, the interpretation of their results remains ambiguous. The application of FT-IR spectroscopy in temperature-dependent regime, along with appropriate spectral treatment and analysis, may enable deciphering the events that drive ripple phase formation on a molecular level.

Temperature-dependent transmission FT-IR spectra, along with DSC measurements, were conducted on lipid multibilayers constituted from 1,2-dipalmitoyl-*sn*-glycero-3-phosphocholine. Lipid multibilayers made from 1,2-dipalmitoyl-*sn*-glycero-3-phosphoethanolamine, which do not form a ripple phase, were examined as a reference. Spectra were analyzed using multivariate curve resolution technique with alternating least squares and evolving factor analysis (MCR-ALS with EFA) and lipid phase transition temperatures were determined.

Polar parts of lipid molecules exert greater response on a ripple phase formation than non-polar ones. However, vibrational signatures of hydrocarbon chains that originate from intramolecular or combined intra- and intermolecular contributions display certain qualitative differences that

pave the way for future work oriented on uncoupling the events that drive ripple phase formation.

Keywords:

1,2-Dipalmitoyl-*sn*-glycero-3-phosphocholine (DPPC); 1,2-Dipalmitoyl-*sn*-glycero-3-phosphoethanolamine (DPPE); Transmission FT-IR spectra, Differential scanning calorimetry; Multivariate curve resolution method; Phase transition(s) temperature(s) assessment; Ripple phase

1. Introduction

Transformation of a lipid bilayer from a solid-ordered phase (gel; L_β) to a liquid-disordered phase (fluid; L_α) is addressed as the main phase transition ($L_\beta \rightarrow L_\alpha$) with a peak at melting point temperature (T_m). Although the most recognizable attribute of this highly energetic, cooperative and fast process is the conformational change of acyl chains from *trans* to *gauche* due to weakening of van der Waals interactions between hydrocarbon chains, hydrogen bonds and charged pairs meshed by lipid polar headgroups and surrounding water molecules contribute the magnitude of T_m [1]. For instance, a network of headgroup-bound water molecules is significantly more ordered for amino headgroups ($-NH_3^+$) of phosphatidylethanolamine (PE) bilayers than for choline headgroups ($-N(CH_3)_3^+$) of phosphatidylcholine (PC) bilayers which merely supports it. When intramolecular hydrogen bonds formed between amino and phosphate groups in PE bilayers are counted in, T_m in PE bilayers are higher than those in PC for the lipids of the same acyl chain types and lengths [2,3].

Homoacyl disaturated PC lipids of certain chain length [4–6]] additionally display $L_{\beta'} \rightarrow P_{\beta'}$ transition, where $P_{\beta'}$ designates ripple phase with characteristic periodic undulations ($P_{\beta'}$) with the ripple length-scale estimated to be between 13-30 nm [7]. This low-cooperativity process of moderate kinetics is usually registered several degrees below the main transition (at T_p; $T_p < T_m$) and is the most prominent in lipid multibilayers [8]. The prime index (') associated with β' refers to the PC chain length- and hydration-dependent tilt of hydrocarbon chains with respect to the lipid bilayer normal in a gel phase as a consequence of the mismatch of cross-sectional areas of polar headgroups and hydrocarbon chains [9]. In contrast to PC lipids, PE lipids are more tightly packed in the bilayer as their amino headgroups are much smaller. Although ordered with a smaller tilt than PC lipids [4], they do not exhibit $P_{\beta'}$ phase so the melting in PE

lipid bilayers follows the path(s) L_c / $L_\beta \rightarrow L_\alpha$ [3]. In the latter L_c designates lamellar crystal phase with more tightly ordered hydrocarbon chains and weakly hydrated polar heads than in L_β phase [8,10].

The attributes of periodic undulations characteristic for 1,2-dimyristoyl-*sn*-glycero-3-phosphocholine (DMPC; di-14:0) and 1,2-dipalmitoyl-*sn*-glycero-3-phosphocholine (DPPC; di-16:0) bilayers were analyzed using various structural analysis techniques, all of which report an asymmetric saw-tooth profile of ripple phase in both DMPC and DPPC [11–13]. Although unified in explaining the asymmetric profile as the coexistence of two domains of different length and thickness (longer and thicker major arm and shorter and thinner minor arm) connected by a kink, the interpretations of the molecular origin of this asymmetry bifurcate. One branch favors the hypothesis that both minor and major arms are built-up from gel-phase lipids, but their explanations of this thickness and length difference vary. As possible causes the change in hydrocarbon chain tilt [14–16], packing pattern [17] or longitudinal displacement of lipid due to increased hydration [4,6] are proposed. Both structural [18] and computational studies suggested the possible impact of lipid interdigitation on thickness of these two domains [19,20]. Another branch advocates that lipids in the major (thicker) arm are in a gel phase, whereas those in minor (thinner) arm exist in fluid phase [5,21–23]. According to the model proposed by Heimburg [5], the melting of individual lipid molecules (gel → fluid) along a line in a triangular lattice induces local bending of a bilayer and results with a periodic pattern of alternating gel and fluid domains. The exceptional success of this model is its ability to predict heat capacity profiles of DPPC bilayers using differential scanning calorimetry (DSC); according to Heimburg, ripple phase formation and lipid melting are parts of the same process which splits into two sub-processes due to simultaneous change in lipid order and curvature [3].

DSC has been successfully applied for decades in registering and characterizing both main- and pretransition of PC-lipid bilayers in the form of liposomes [2,3,24,25]. These endothermal processes are observed as deviations from the baseline on a DSC curve, being a function of both kinetic and thermotropic properties of particular phase transition. Although this technique does not provide any information regarding molecular-level events, its operational simplicity and efficiency in registering lipid phase transitions, along with providing desirable physicochemical quantities, are appreciable advantages of this thermoanalytical technique [26–28]. Major drawback related with DSC concerns thermal history of the sample; depending on the sample storage and its pretreatment, features of certain phase transitions observed in the first heating run can deviate from those observed in the second one (and eventual subsequent

runs). Therefore, the second heating run is commonly taken as a representative DSC curve of the lipid bilayer under investigation [27]. This issue is especially mirrored in the characterization of both main transition and pretransition; the former is manifested as a relatively strong and narrow curve on a DSC profile and is relatively independent on previous sample treatment, whereas the latter one generates much weaker and broader curve and is more sensitive to both sample treatment and measurement conditions [29].

In contrast to thermal properties, molecular picture of the melting process usually refers to the loss in hydrocarbon chain order which is manifested as *trans* to *gauche* conformational change of lipid methylene groups (CH_2). Changes in these structural features are straightforwardly revealed by FT-IR spectroscopy [30]. In particular, CH_2 groups produce bands that are strong enough and distinguishable from a very strong and broad vibrational feature generated by the stretching of OH groups (νOH) of water. When lipid bilayer undergoes gel → fluid phase transition (at T_m), the signals of symmetric ($\nu_s CH_2$) and antisymmetric ($\nu_{as} CH_2$) stretching of CH_2 groups displace to the higher wavenumbers for about 4 cm^{-1}. Moreover, a steep decrease in the band absorbance accompanies this displacement. In the simplest form, temperature dependence of the band position usually produces a sigmoid curve with the inflection point corresponding to the main phase transition temperature (T_m) [31]. FT-IR spectroscopy was occasionally employed in the assessment of T_p of DPPC multibilayers; by analyzing temperature-dependent changes in the position, absorbance or full width at half maximum of the bands that originate from vibrations of methylene, phosphate or carbonyl groups, Cameron et al. concluded that pretransition rises due to the change of a packing pattern of hydrocarbon chains [17]. This finding was later questioned by Le Bihan and Pézolet who suggested that a decrease in the tilt of hydrocarbon chains with respect to the bilayer normal and subsequent bilayer swelling drives ripple phase formation [15].

Contrary to the discussed results, which were usually oriented on the analysis of particular vibrational signature at a single point, methods based on a simultaneous analysis of a dataset that encompasses spectral range(s) with the purpose of determining phase transition temperature can be applied as well. For instance, multivariate curve resolution with alternating least squares (MCR-ALS) and evolving factor analysis (EFA) [32–34] was already applied in the determination of T_m and T_p of DPPC liposomes [35]. This study revealed that the main transition is associated with the changes in vibrational signatures of methylene groups, whereas structural rearrangement of polar groups was found to be intimately related with the pretransition. However, we suspect that certain details of the previously performed analysis

were gravely overlooked and, consequently, portion of the obtained results, especially those related to T_p determination, were misinterpreted. In order to present the correct application of MCR-ALS with EFA in the assessment of lipid bilayers phase transition temperatures, we have examined multilamellar liposomes of DPPC (Fig. 1) in NaCl solution (I = 100 mM) [1,12] using temperature-dependent FT-IR spectroscopy and DSC. Furthermore, ability to determine T_p via analysis of vibrational signatures of various parts of lipid molecules or, respectively, those affected by the changes in the arrangement of lipid molecules, demonstrates the potential of MCR-ALS with EFA in uncoupling the events that drive ripple phase formation. Multilamellar aggregates of DPPE (Fig. 1) in NaCl solution, used as a reference system that does/should not display pretransition, were explored in the same manner. Discrepancies in T_m obtained from DSC and FT-IR spectroscopy for DPPE multibilayers were additionally discussed.

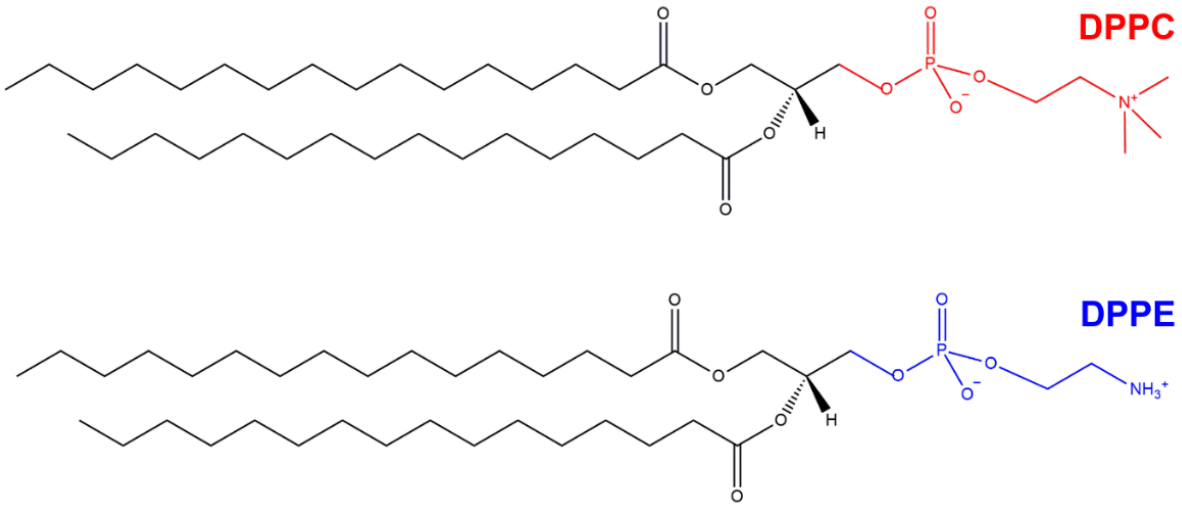

Fig. 1. Structural formulas of 1,2-dipalmitoyl-*sn*-glycero-3-phosphocholine (DPPC – red headgroup) and 1,2-dipalmitoyl-*sn*-glycero-3-phosphoethanolamine (DPPE – blue headgroup)

2. Experimental

2.1 Chemicals and suspensions preparations

1,2-Dipalmitoyl-2-sn-glycero-3-phosphocholine (DPPC; white powder) and 1,2-dipalmitoyl-2-sn-glycero-3-phosphoethanolamine (DPPE; white powder) was purchased from Avanti Polar Lipids (≥ 99 %) and Cayman Chemical (≥ 98 %), respectively, and used as received. A water solution of NaCl (prepared from NaCl (Kemika, p. a. grade) and milli-Q water) of ionic strength (concentration) I = 100 mM and pH ~ 5 was used as a hydrating agent.

In order to make multilamellar liposome (aggregate) suspension, approximately 25 mg of DPPC (DPPE) was dissolved in 500 μl (1000 μl) of NaCl solution (100 mM). The samples were vortexed for several minutes, placed in a H_2O bath, heated up to 80 °C, where they were held for 2 minutes. Vortexing and heating of the sample were repeated for at least two more times. The size of thus prepared liposomes was determined using dynamic light scattering (DLS); the hydrodynamic diameter (d_h) for DPPC liposomes at 30 °C is found to be $d_h \approx 3\mu m$ and for DPPE multilamellar aggregates at 52 °C we found $d_h \sim 200$ nm (detailed information regarding DLS measurements is given in Supporting Information, section S1).

2.2 FT-IR spectroscopy

2.2.1 FT-IR spectra acquisition

FT-IR spectra were measured on an ABB Bomem MB102 spectrometer, equipped with CsI optics and a DTGS detector in a transmission. DPPC and DPPE liposome suspensions, as well as NaCl solution, were recorded in a sealed cell equipped with CaF_2 windows with the path length of the cell $d = 27.37$ μm which was determined interferometrically. Temperature was regulated by Specac 3000 Series high stability temperature controller with heating jacket. DPPC and DPPE liposome dispersions were recorded in the temperature range 30 – 52 °C and 53 – 75 °C, respectively. The heating rate was 1 °C min^{-1}. Every sample was recorded as two independent cell fillings (except for NaCl solution which was recorded once), with each cell filling heated twice (heating – cooling – heating – cooling) in order to make measurements analogous to DSC (see subsection 2.3). Subsequent analysis will give an insight into eventual differences between these two runs. All spectra were collected with nominal resolution of 2 cm^{-1} and 10 scans.

2.2.2 FT-IR spectra analysis

FT-IR spectra are analyzed using MCR-ALS, which is a mathematical method enabling isolation and quantification of the main sources of variation in a data set, in turn decomposing the measured system (in this case, spectra) into subcomponents. However, MCR-ALS analysis demands proper initial conditions to produce meaningful results, i.e. one needs to provide it with the initial guess of contributions of different components underlying the investigated system. EFA method can be readily used to accomplish the latter, the results of which serve as a starting point of MCR-ALS analysis [34]. In the following short preliminary preparation of

the obtained data/spectra will be presented, and basis of EFA and MCR-ALS analysis will be explained.

After measuring FT-IR spectra of DPPC and DPPE suspensions in their respective temperature ranges, a data pretreatment was performed. Firstly, obtained spectra were divided into four separate spectral regions (D_1-D_4) in which vibrational signatures of lipid molecules are the most prominent: i) 2880 – 2824 cm^{-1} (symmetric stretching of methylene (CH_2) group; ν_sCH_2), ii) 1800 – 1690 cm^{-1} (stretching of carbonyl (CO) group: νCO that partially overlap with water linear bending δHOH), iii) 1515 – 1427 cm^{-1} and 1485 – 1427 cm^{-1} for DPPC and DPPE, respectively (scissoring of methylene (CH_2) group; γCH_2), and iv) 1273 – 1190 cm^{-1} (antisymmetric stretching of PO_2^- group; $\nu_{as}PO_2^-$). Additionally, a spectral region 2620 – 1865 cm^{-1} (D_5) where only water absorbs (a combination band that originates from water bending and water libration (δHOH+H_2O libration); H_2O comb) was included as well. As it serves both as a reference and a guide to the behavior of the analysis itself when no underlying component exhibits phase transition, this band was examined in FT-IR spectra of NaCl solution in aforementioned temperature ranges as well (Supporting Information, section S2, Figs. S1 and S2). These five spectral regions constitute five distinct data matrices (**D_1**-**D_5**) in which each data matrix contains in rows its respective frequency range of measured spectra. Furthermore, each obtained matrix possesses the same number of rows (N_r), where N_r is the number of spectra measured at successive temperatures (in this study $N_r = 23$), while the number of columns varies with the number of wavenumbers (ν_m) measured in the corresponding region. Thus, dimensions of the prepared matrices are $N_r \times \nu_m$, respectively. Secondly, the chosen spectral ranges were baseline corrected. The subsequent analysis (EFA and MCR-ALS) of the five described regions was accomplished using the publicly available Matlab-code [36].

Before venturing into EFA, the initial number of components in the investigated system is accomplished using singular value decomposition (SVD). With the *a priori* knowledge of the number of components that contribute to the overall spectrum in the investigated system, the chosen number of components after SVD analysis was always set to 2, corresponding to the lipid molecules found in either gel or a fluid phase. This assumption was also substantiated by the obtained singular values corresponding to the first two eigenvectors obtained after SVD. Upon finding the initial number of components via SVD analysis, the constructed data matrix can be analyzed employing EFA [34,37]. This method can be thought of as a "propagating" singular value decomposition of a matrix $\mathbf{D_i}$ (with **i**=**1**, **2**, ..., **5**), applied to submatrices of $\mathbf{D_i}$

built up by adding the rows of $\mathbf{D_i}$ successively. The procedure is carried out in two directions, namely forward (1, 2, 3, …, N_r rows), starting with the two first spectra/rows and adding them in the direction of the experiment (thus forward), and backward (N_r, N_r - 1, N_r - 2, …, 1 rows), starting with the last two spectra/rows. Proper combination of the information gathered from forward and backward curves provides a first estimation of the concentration profiles of the individual components present in the system. This first estimate of the concentration profiles is then used as a starting point of the iterative process in the MCR-ALS procedure.

Finally, having estimated the initial concentration profiles via EFA, MCR-ALS optimization can be used to recover a physically meaningful set of concentration profiles and spectra of every individual species, in such way to best explain the variance present in the data. Importantly, this procedure hangs on the premise that the data matrix is bilinear, i.e. that it can be decomposed as the product of two matrices. The decomposition of the data matrix D can be performed according to the following equation:

$$\mathbf{D} = \mathbf{C}\mathbf{S}^{\mathbf{T}} + \mathbf{E},$$

with $\mathbf{S}^{\mathbf{T}}$ representing the matrix of individual pure spectra, **C** is the matrix of the concentration profiles, whereas **E** represents the matrix of residuals unexplained by species present in **C** and $\mathbf{S}^{\mathbf{T}}$. Since the analyzed data matrices correspond to IR spectra, several constraints were applied during MCR-ALS procedure; both concentration and spectral profiles were imposed to be positive using non-negativity constraint, with unimodality constraints being applied to both individual pure spectra.

The appearance of concentration profiles significantly depends on the chosen spectral region and on the chemical species that produces signatures in the chosen spectral region. In the absence of a compound that undergoes a phase transition, inherently linear concentration profiles are to be observed. On the contrary, when examined spectral window contains the signature of a species experiencing a phase transition in examined temperature range, concentration profiles with sigmoid-like features are expected [35] as any phase transition is bound to show a discontinuous change in the systems response [3] (described in detail in Supporting Information, sections S2 and S3). Thus, a careful choice and spectral treatment of the analyzed spectral region, along with the correct interpretation of the observed results of MCR-ALS with EFA, enables a clear distinction between the effects that arise from the change in macroscopic properties of a solution (refractive index, in particular) [38–40] and those that

are the result of the phase transition change of solute molecules [41,42] (Supporting Information, section S3, Figs. S3, S4).

Further in the text (from section 3. Results and Discussion) particular component (with associated concentration profiles) will be addressed as a low-temperature component and a high-temperature component. The former one refers to the lipid specie that exists at temperatures below T_m (gel-phase lipid molecule), whereas the latter one denotes the lipid specie found at temperatures above T_m (fluid-phase lipid molecule). Details on statistical analysis associated with MCR-ALS with EFA are given in Supporting Information, section S4. Moreover, each of the two components elucidated via MCR-ALS comes with its associated spectral profile that will be displayed along with the experimentally acquired FT-IR spectra.

2.3 DSC: suspensions preparation and thermal analysis

The DPPC and DPPE suspensions for DSC measurements were prepared similarly as for the FT-IR measurements except for the concentration, which was about 5 mg ml^{-1}. Samples were held for 15 minutes in a degassing station before they were placed in the cell and measured.

The calorimetric experiments were carried out in a microcalorimeter Nano-DSC, TA Instruments (New Castle, USA) at a scan rate of 1 °C min^{-1}, temperature range 20-80 °C and cell volume of 300 µL. Data analysis was done using the TA Instruments Nano Analyze software package. Both DPPC and DPPE suspensions were recorded two times (two independent fillings) in two heating & cooling cycles. The reference solution–reference solution (NaCl in water–NaCl in water) scan was collected once in two heating & cooling cycles (as samples spectra) and subtracted from the raw samples data. The baseline was manually constructed and subtracted from the resultant curve. T_m (and T_p) are determined from the onset, the reading of which is independent on the applied heating rate [43], of the thermal history-unburdened second heating run (DSC profiles obtained in the first heating run are displayed in Supporting Information, section S5, Fig. S5).

3. Results and Discussion

FT-IR spectra of multilamellar DPPC liposomes and multilamellar DPPE aggregates in water solution of NaCl (I = 100 mM) are displayed in Fig. 2a-h (FT-IR spectra designated with solid lines). Regardless of the functional group that generates a specific signal (methylene, carbonyl or phosphate group), the temperature rise is accompanied by the decrease in the intensity of observed vibrational signatures. More importantly, absorbance of the bands assigned to the

normal modes $\nu_s CH_2$, γCH_2 and $\nu_{as} PO_2^-$ displays abrupt decrease at the temperature(s) at which phase transition(s) are expected (Fig. 2a, b, e-h) [31]. On the contrary, unambiguous discontinuities in νCO spectral range (Fig. 2b, c) are not observed. A major cause of their apparent absence is the significant overlap between νCO band and much stronger water signal (H_2O bending; δHOH), with the maximum usually occurring at approximately 1640 cm^{-1} [30]. Although this issue might be tentatively resolved by subtracting the spectrum of NaCl water solution from the spectrum of a suspension, we did not apply this approach. (In Supporting Information (section S3, Fig. S4) it is demonstrated that (unnecessary) subtraction of the solvent introduces additional uncertainties and ambiguities where ones should not be). Instead, FT-IR spectral ranges containing signatures of both water and lipid molecules are examined analogously to FT-IR spectral ranges in which only lipid molecules absorb.

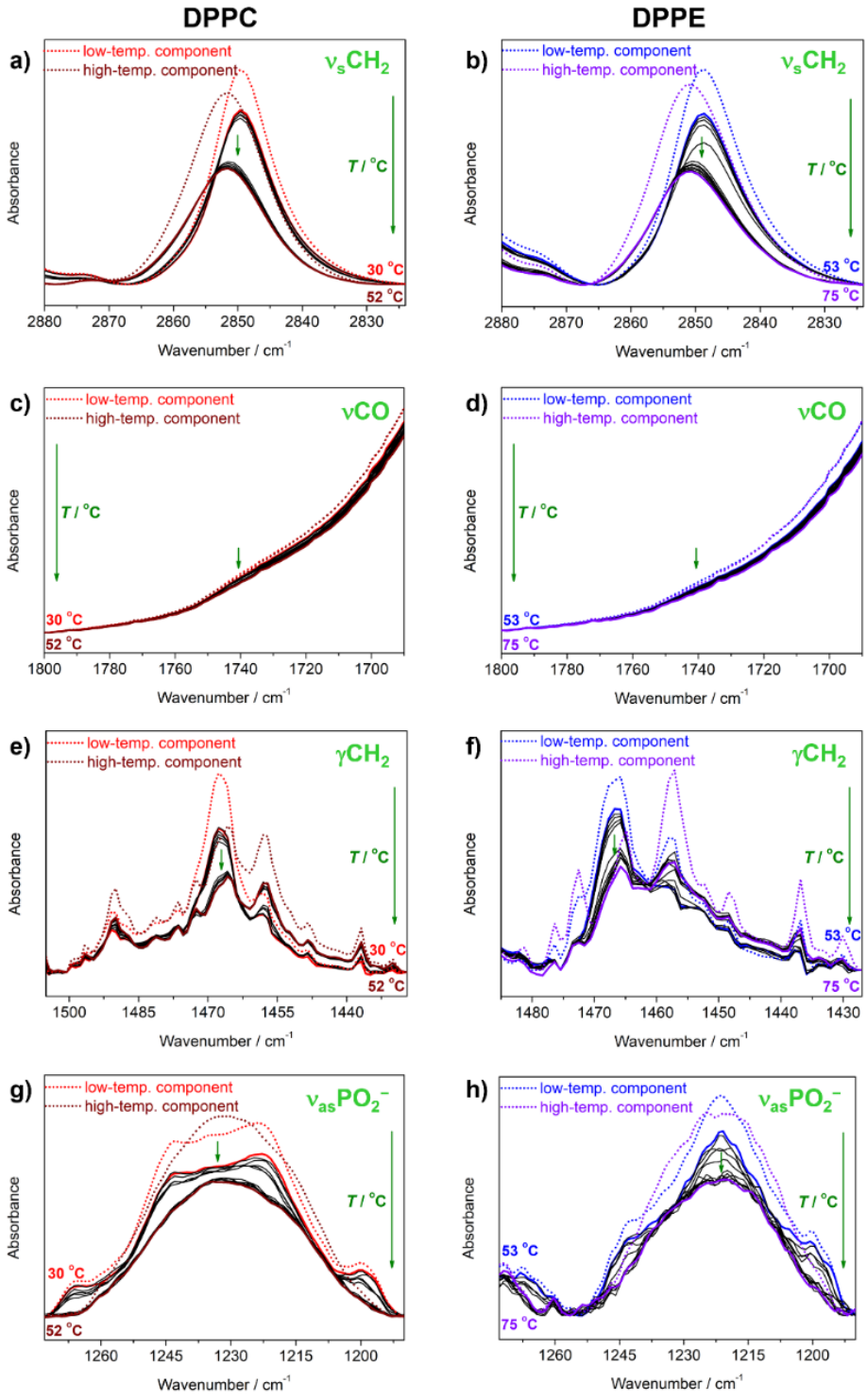

Fig. 2. Selected spectral ranges of temperature-dependent FT-IR spectra of DPPC liposomes (left column) and DPPE aggregates (right column) labelled with solid lines: a) $\nu_s CH_2$ in DPPC; b) $\nu_s CH_2$ in DPPE; c) νCO in DPPC; d) νCO in DPPE; e) γCH_2 in DPPC; f) γCH_2 in DPPE; g) $\nu_{as} PO_2^-$ in DPPC; h) $\nu_{as} PO_2^-$ in DPPE. The lowest and the highest temperatures are highlighted: 30 °C (red) and 52 °C (wine) for DPPC and 53 °C (blue) and 75 °C (violet) for DPPE. Dotted

lines refer to the FT-IR spectra of low- and high-temperature components obtained using MCR-ALS with EFA (DPPC: red for low- and wine for high-temperature component; DPPE: blue for low- and violet for high-temperature component).

When analyzing temperature-dependent FT-IR spectra of DPPC and DPPE suspension in the first heating runs in selected spectral ranges using MCR-ALS with EFA, concentration profiles of low- and high-temperature components with sigmoidal dependency on temperature are obtained; low-temperature component displays a decrease with increase in temperature, whereas high-temperature component displays an opposite trend (Fig. 3a-h). (performed analysis revealed that T_m and T_p values coincide within experimental uncertainty regardless of the heating run, thus only results of the first heating run are displayed in the main text, with second heating run results available in Supporting Information, Section S6, Fig. S6, Table S3).

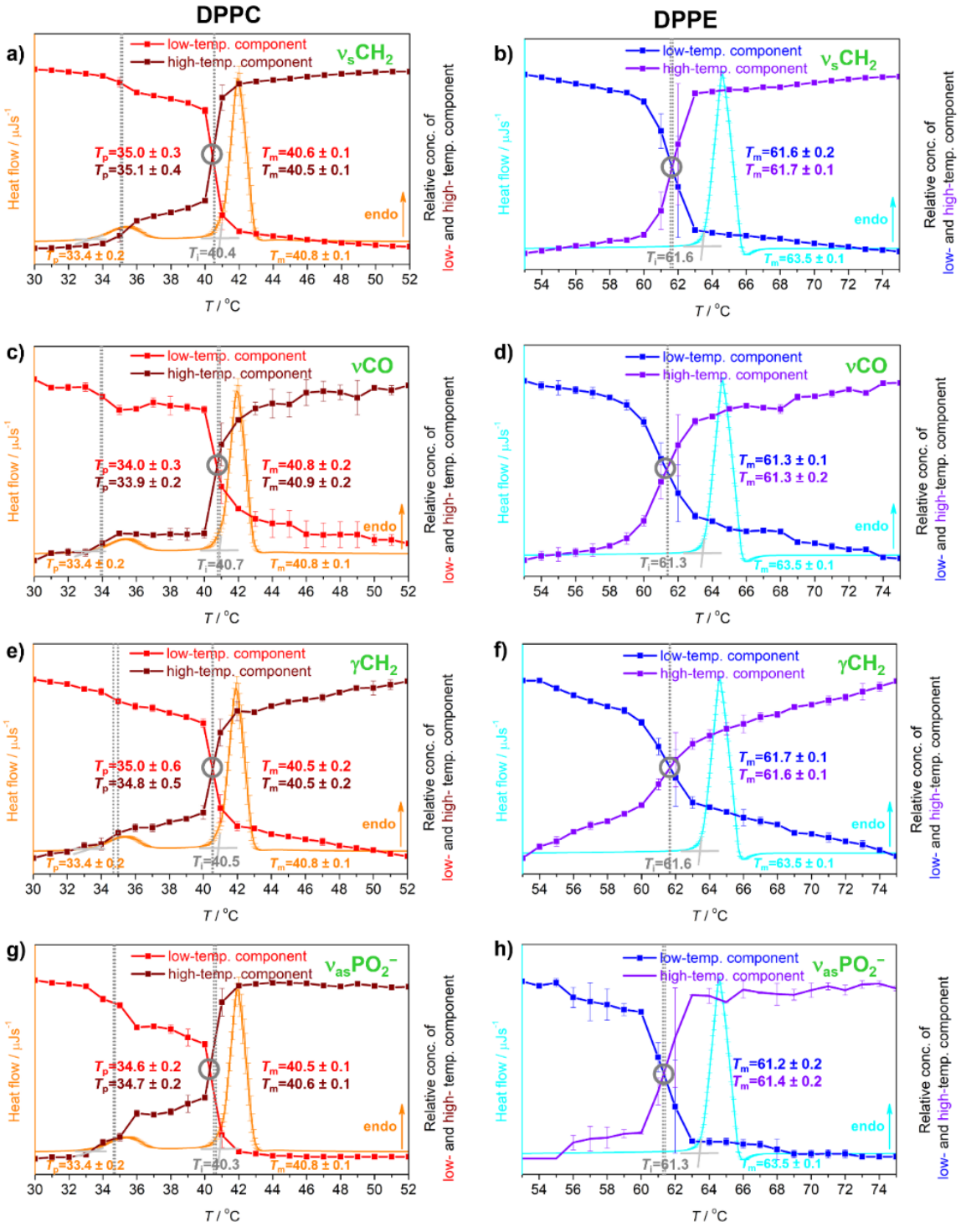

Fig. 3. Concentration profiles of low- and high-temperature components of DPPC liposomes (left column) and DPPE aggregates (right column) collected in the first heating run, along with their DSC curves obtained in the second heating run, in four spectral regions: a) $\nu_s CH_2$ in DPPC; b) $\nu_s CH_2$ in DPPE; c) νCO in DPPC; d) νCO in DPPE; e) γCH_2 in DPPC; f) γCH_2 in DPPE; g) $\nu_{as} PO_2^-$ in DPPC; h) $\nu_{as} PO_2^-$ in DPPE. DPPC and DPPE columns contain, respectively,

concentration profiles of low- (red and blue) and high-temperature components (wine and violet) obtained from the temperature-dependent FT-IR spectra acquired in the first heating run, along with DSC curve (orange and cyan) obtained in the second heating run. T_m (and T_p) values obtained using MCR-ALS with EFA applied on temperature-dependent FT-IR spectra and from DSC measurements are displayed on figures with the corresponding color. The intersection point is labelled gray for both DPPC and DPPE in all four spectral ranges (see Table 1).

Regarding DPPC liposomes, both components in all four explored spectral ranges display double sigmoid transition: one at lower temperatures and one significantly steeper found about the middle of the explored temperature range. Inflection points of these sigmoidal transitions correspond to, respectively, T_p and T_m (details on how inflection points are evaluated can be found in Supporting Information, section S4). In particular, T_p values obtained from, respectively, low- and high-temperature components are: 35.0 ± 0.3 °C and 35.1 ± 0.4 °C (ν_sCH_2), 34.0 ± 0.3 °C and 33.9 ± 0.2 °C (νCO), 35.0 ± 0.6 °C and 34.8 ± 0.5 °C (γCH_2), and 34.6 ± 0.2 °C and 34.7 ± 0.2 °C ($\nu_{as}PO_2^-$) (see Table 1). The average T_p is determined as a standard deviation of all listed values (T_p = 35 ± 1 °C) and slightly differs from the value obtained from DSC curve (T_p = 33.4 ± 0.2 °C). This discrepancy might arise due to challenging determination of the inflection point of rather broad and shallow sigmoid transition. This issue is especially expressed in spectral ranges ν_sCH_2 or γCH_2 (Fig. 3a and 3c) where the sigmoid transition is much less pronounced than in spectral ranges νCO or $\nu_{as}PO_2^-$, implying that analyzed vibrational signatures unequally respond to the ripple phase appearance. Furthermore, although average T_p is determined from four equally weighted *T*p's and all *T*p's coincide within the limits of the uncertainty, T_p measured from νCO range is apparently at the lower end of T_p value span, in contrast to the analogous value assessed from ν_sCH_2 or γCH_2 (Table 1). Potential deviations of T_p values obtained from all four spectral ranges might suggest either which portion of lipid molecule is more affected by this pretransition or whether certain part of the lipid experiences the pretransition at slightly different temperature. Accordingly, methylene groups of hydrocarbon chains might probe ripple phase formation as well as (much more) solvent-exposed carbonyl and phosphate moieties. However, their response is comparably reduced due to minimally disturbed hydrocarbon chain packing or interchain interactions at T_p (Fig. 3a, c) [30]. Alternatively, different parts of lipid molecules (methylene, carbonyl and phosphate moieties) might participate in ripple phase formation not at particular T_p but in certain temperature interval. In turn, the thermodynamics and kinetics of the ripple phase formation in applied experimental conditions (heating rate of 1 °C min^{-1}) might prevent more accurate

assignment of T_p, emphasizing the eventual differences in observed T_p values obtained from different spectral regions, i.e. different parts of lipids.

T_m values obtained from, respectively, low- and high-temperature components are: 40.6 ± 0.1 °C and 40.5 ± 0.1 °C ($\nu_s CH_2$), 40.8 ± 0.2 °C and 40.9 ± 0.2 °C (νCO), 40.5 ± 0.2 °C and 40.5 ± 0.2 °C (γCH_2), and 40.5 ± 0.1 °C and 40.6 ± 0.1 °C ($\nu_{as} PO_2^-$). Their average value (T_m = 40.7 ± 0.3 °C) is in excellent agreement with analogous quantity determined from a DSC curve (T_m = 40.8 ± 0.1 °C) (see Table 1).

In DPPE aggregates only one inflection point (one sigmoid transition) is observed in all four spectral ranges, its position corresponding to T_m. The values obtained from sigmoid transitions in concentration profiles of, respectively, low- and high-temperature components are: 61.6 ± 0.2 °C and 61.7 ± 0.1 °C ($\nu_s CH_2$), 61.3 ± 0.1 °C and 61.3 ± 0.2 °C (νCO), 61.7 ± 0.1 °C and 61.6 ± 0.1 °C (γCH_2), and 61.2 ± 0.2 °C and 61.4 ± 0.2 °C ($\nu_{as} PO_2^-$). Their average value (T_m = 61.5 ± 0.4 °C) deviates from the corresponding value obtained from DSC measurements (T_m = 63.5 ± 0.1 °C) for about 2 °C (see Table 1). Although discrepancy in T_m of DPPE obtained by different techniques is already reported [10], to the best of our knowledge this phenomenon is yet to be explained. Since analogous phenomenon is not observed in DPPC multibilayers, we suggest that this deviation in DPPE multibilayers arises due to distinct heat transfer between water and polar lipid headgroups of DPPE (in contrast to DPPC). In this respect, water forms clathrate structure around choline moiety in PC lipids [44,45]. On the other hand, water molecules are able to establish direct contacts with an amino group of PE [46], resulting with differently ordered water structure around PE and PC headgroups [47,48]. As liposomes composed from PE lipids are generally less hydrated than those made of PC lipids [49], it is expected that both water and lipid headgroups in the former are more oriented than in the latter one. Our ongoing computational and calorimetric research may shed light on a difference in water arrangement impact on melting of DPPC and DPPE multibilayers.

Table 1. Phase transition temperatures (T_{pt}) for DPPC (T_m and T_p) and DPPE (T_m) obtained by DSC and FT-IR spectroscopy using MCR-ALS with EFA

system		T_{pt} / °C					
		DSC	FT-IR				
			ν_sCH_2	νCO	γCH_2	$\nu_{as}PO_2^-$	average
DPPC	T_m	**40.8 ± 0.1**	40.6 ± 0.1	40.8 ± 0.2	40.5 ± 0.2	40.5 ± 0.1	**40.7 ± 0.3**
			40.5 ± 0.1	40.9 ± 0.2	40.5 ± 0.2	40.6 ± 0.1	
			40.4	*40.7*	*40.5*	*40.3*	*40.5 ± 0.2*
	T_p	**33.4 ± 0.2**	35.0 ± 0.3	34.0 ± 0.3	35.0 ± 0.6	34.6 ± 0.2	**35 ± 1**
			35.1 ± 0.4	33.9 ± 0.2	34.8 ± 0.5	34.7 ± 0.2	
DPPE	T_m	**63.5 ± 0.1**	61.6 ± 0.2	61.3 ± 0.1	61.7 ± 0.1	61.2 ± 0.2	**61.5 ± 0.4**
			61.7 ± 0.1	61.3 ± 0.2	61.6 ± 0.1	61.4 ± 0.2	
			61.6	*61.3*	*61.6*	*61.3*	*61.5 ± 0.2*

As MCR-ALS with EFA applied on FT-IR spectra of DPPC and DPPE in two heating runs revealed that T_m (and T_p) values coincide within experimental uncertainty, the data obtained from the second heating run are displayed in Supporting Information (Section S6, Fig. S6, Table S3).

Nevertheless, concentration profiles of low- and high-temperature components of both DPPC and DPPE intersection at a point coincided with T_m of the respective lipid: 40.4 °C (ν_sCH_2), 40.7 °C (νCO), 40.5 °C (γCH_2), and 40.3 °C ($\nu_{as}PO_2^-$) for DPPC (on average 40.5 ± 0.2 °C) and, respectively, 61.6 °C (ν_sCH_2), 61.3 °C (νCO), 61.6 °C (γCH_2), and 61.3 °C ($\nu_{as}PO_2^-$) for DPPE (on average 61.5 ± 0.2 °C) (italics in Fig. 3a-h and in Table 1). Since lipid molecules undergo the transformation from the gel to the fluid phase at T_m, this rationale implies that at temperatures below intersection point lipids are in the gel phase, whereas above intersection point in the fluid phase. Accordingly, the ripple phase of DPPC ($T_p < T_m$) is, therefore, built-up from only gel-phase lipids. Comparing the steepness and the magnitude of sigmoid transition associated with the ripple phase formation in four examined spectral ranges in qualitative terms (Fig. 3a, c, e, g), polar moieties (phosphate and carbonyl) probe ripple phase much more than hydrocarbon chains. This greater sensitivity might arise due to greater hydration of polar groups at pretransition. Spectral response of the hydrocarbon chain during ripple phase formation may contain an exceptional piece of information since, in strictly qualitative terms, ν_sCH_2 (an intramolecular feature) apparently exerts slightly greater response than γCH_2 (Fig. 3a, c). As the latter reflects both *trans* → *gauche* conformation change of methylene groups an

(intramolecular feature) and lipid ordering (intermolecular feature) [29], it might be that lipid ordering is not significantly affected by the appearance of periodic undulations. In this context, our results might be viewed as a support of Cevc's theory according to which increased solvation of polar moieties, and partial interdigitation of hydrocarbon chains due to their longitudinal displacement induces ripple phase [50].

4. Conclusion

The phase transition(s) temperature(s) of DPPC multilamellar liposomes (T_m and T_p) and DPPE multilamellar aggregates (T_m) in NaCl water solution were determined from their temperature-dependent transmission FT-IR spectra using MCR-ALS with EFA and from DSC. Correct application of this multivariate curve resolution method enabled the determination of T_m's (and of T_p) from all spectral ranges in which vibrational signatures of lipid molecules appear. The analysis of signals generated by various parts of lipid molecules clearly suggests that, using MCR-ALS with EFA, the events that drive less cooperative phase transitions (such as pretransition) might be resolved. The application of MCR-ALS with EFA in more detailed characterization of ripple phase features is underway. A discrepancy in T_m of DPPE found via spectroscopic and DSC measurements is briefly discussed in terms of water ordering impact as an introduction to the research in progress.

Acknowledgment

This paper was supported by the Croatian Science Foundation, Project Nos. UIP-2014-09-6090, IP-2019-04-3804 and IP-2018-01-5475. The authors gratefully acknowledge Prof. Dr. Matthias P. Mayer (Ruprecht-Karls-University Heidelberg, Center for Molecular Biology, Heidelberg, Germany) and Excellence cluster CellNetworks for utilizing the FT-IR spectrometer with ATR unit, Mr. Stanislav Martin (LKB Vertriebs Ges.m.b.H.) who enabled the access on the Zetasizer Ultra (Malvern Panalytical, UK) and Dr. Atiđa Selmani (Laboratory for biocolloids and surface chemistry, Ruđer Bošković Institute) for making DLS measurements. D.B. acknowledges Dr. Mario Vazdar (Laboratory for chemistry in model biological systems, Ruđer Bošković Institute) for helpful discussions and constructive advices in manuscript preparation and Dr. Suzana Šegota (Laboratory for biocolloids and surface chemistry, Ruđer Bošković Institute) for providing instrumental support.

Supporting Information

Supporting Information associated with this paper can be found in the online version at http://.

References:

[1] D. Marsh, Structural and thermodynamic determinants of chain-melting transition temperatures for phospholipid and glycolipids membranes, Biochim. Biophys. Acta - Biomembr. 1798 (2010) 40–51. doi:10.1016/j.bbamem.2009.10.010.

[2] J.M. Seddon, G. Cevc, D. Marsh, Calorimetric studies of the gel-fluid (L_β-L_α) and lamellar-inverted hexagonal (L_α-H_{II}) phase transitions in dialkyl- and diacylphosphatidylethanolamines, Biochemistry. 22 (1983) 1280–1289. doi:10.1021/bi00274a045.

[3] T. Heimburg, Thermal Biophysics of Membranes, First, Wiley-VCH Verlag GmbH & Co, Weinheim, 2007.

[4] G. Cevc, How Membrane Chain-Melting Phase-Transition Temperature Is Affected by the Lipid Chain Asymmetry and Degree of Unsaturation: An Effective Chain-Length Model, Biochemistry. 30 (1991) 7186–7193. doi:10.1021/bi00243a021.

[5] T. Heimburg, A model for the lipid pretransition: Coupling of ripple formation with the chain-melting transition, Biophys. J. 78 (2000) 1154–1165. doi:10.1016/S0006-3495(00)76673-2.

[6] B.A. Cunningham, A.D. Brown, D.H. Wolfe, W.P. Williams, A. Brain, Ripple phase formation in phosphatidylcholine: Effect of acyl chain relative length, position, and unsaturation, Phys. Rev. E - Stat. Physics, Plasmas, Fluids, Relat. Interdiscip. Top. 58 (1998) 3662–3672. doi:10.1103/PhysRevE.58.3662.

[7] T. Kaasgaard, C. Leidy, J.H. Crowe, O.G. Mouritsen, K. Jørgensen, Temperature-Controlled Structure and Kinetics of Ripple Phases in One- and Two-Component Supported Lipid Bilayers, Biophys. J. 85 (2003) 350–360. doi:10.1016/S0006-3495(03)74479-8.

[8] R. Koynova, M. Caffrey, Phases and phase transitions of the phosphatidylcholines, Biochim. Biophys. Acta. 1376 (1998) 91–145. doi:10.1016/S0013-4686(03)00208-1.

[9] S. Tristram-Nagle, R. Zhang, R.M. Suter, C.R. Worthington, W.J. Sun, J.F. Nagle, Measurement of chain tilt angle in fully hydrated bilayers of gel phase lecithins, Biophys. J. 64 (1993) 1097–1109. doi:10.1016/S0006-3495(93)81475-9.

[10] R. Koynova, M. Caffrey, Phases and phase transitions of the hydrated phosphatidylethanolamines, Chem. Phys. Lipids. 69 (1994) 1–34. doi:10.1016/S0304-4157(98)00006-9.

[11] M.J. Janiak, D.M. Small, G.G. Shipley, Temperature and Compositional Dependence of the Structure of Hydrated Dimyristoyl Lecithin, J. Biol. Chem. 254 (1979) 6068–6078.

[12] W.Q. Sun, A.C. Leopold, L.M. Crowe, J.H. Crowe, Stability of dry liposomes in sugar glasses., Biophys. J. 70 (1996) 1769–76. doi:10.1016/S0006-3495(96)79740-0.

[13] D.C. Wack, W.W. Webb, Synchrotron x-ray study of the modulated lamellar phase P_{β}' in the lecithin-water system, Phys. Rev. A. 40 (1989) 2712–2730. doi:10.1017/CBO9781107415324.004.

[14] M.P. Hentschel, F. Rustichelli, Structure of the Ripple Phase P in Hydrated Phosphatidylcholine Multimembranes, Phys. Rev. Lett. 66 (1991) 903–906. doi:10.1103/PhysRevLett.66.903.

[15] T. Le Bihan, M. Pézolet, Study of the structure and phase behavior of dipalmitoylphosphatidylcholine by infrared spectroscopy: Characterization of the pretransition and subtransition, Chem. Phys. Lipids. 94 (1998) 13–33. doi:10.1016/S0009-3084(98)00022-X.

[16] K. Sengupta, V.A. Raghunathan, J. Katsaras, Novel structural features of the ripple phase of phospholipids, Europhys. Lett. 49 (2000) 722–728. doi:10.1209/epl/i2000-00210-x.

[17] D.G. Cameron, H.L. Casal, H.H. Mantsch, Characterization of the Pretransition in 1,2-Dipalmitoyl-*sn*-Glycero-3-Phosphocholine by Fourier Transform Infrared Spectroscopy, Biochemistry. 19 (1980) 3665–3672. doi:10.1021/bi00557a005.

[18] K. Akabori, J.F. Nagle, Structure of the DMPC lipid bilayer ripple phase, Soft Matter. 11 (2015) 918–926. doi:10.1039/c4sm02335h.

[19] O. Lenz, F. Schmid, Structure of Symmetric and Asymmetric " Ripple " Phases in Lipid Bilayers, Phys. Rev. Lett. 98 (2007) 058104. doi:10.1103/PhysRevLett.98.058104.

[20] A.H. De Vries, S. Yefimov, A.E. Mark, S.J. Marrink, Molecular structure of the lecithin ripple phase, Proc. Natl. Acad. Sci. U. S. A. 102 (2005) 5392–5396. doi:10.1073/pnas.0408249102.

[21] M. Rappolt, G. Pabst, G. Rapp, M. Kriechbaum, H. Amenitsch, C. Krenn, S. Bernstorff, P. Laggner, New evidence for gel-liquid crystalline phase coexistence in the ripple phase of phosphatidylcholines, Eur. Biophys. J. 29 (2000) 125–133. doi:10.1007/s002490050257.

[22] W.J. Sun, S. Tristram-Nagle, R.M. Suter, J.F. Nagle, Structure of the ripple phase in lecithin bilayers, Proc. Natl. Acad. Sci. U. S. A. 93 (1996) 7008–7012. doi:10.1073/pnas.93.14.7008.

[23] K.A. Riske, R.P. Barroso, C.C. Vequi-Suplicy, R. Germano, V.B. Henriques, M.T. Lamy, Lipid bilayer pre-transition as the beginning of the melting process, Biochim. Biophys. Acta - Biomembr. 1788 (2009) 954–963. doi:10.1016/j.bbamem.2009.01.007.

[24] C. Demetzos, Differential Scanning Calorimetry (DSC): a Tool to Study theThermal Behavior of Lipid Bilayers and Liposomal Stability, J. Liposome Res. 18 (2008) 159–173. doi:10.1080/08982100802310261.

[25] M.H. Chiu, E.J. Prenner, Differential scanning calorimetry: An invaluable tool for a detailed thermodynamic characterization of macromolecules and their interactions, J. Pharm. Bioallied Sci. 3 (2011) 39–59. doi:10.4103/0975-7406.76463.

[26] M. Fidorra, T. Heimburg, H.M. Seeger, Melting of individual lipid components in binary lipid mixtures studied by FTIR spectroscopy, DSC and Monte Carlo simulations, Biochim. Biophys. Acta - Biomembr. 1788 (2009) 600–607. doi:10.1016/j.bbamem.2008.12.003.

[27] C. Chen, D. Han, C. Cai, X. Tang, An overview of liposome lyophilization and its future potential, J. Control. Release. 142 (2010) 299–311. doi:10.1016/j.jconrel.2009.10.024.

[28] D. Bakarić, D. Carić, K. Vazdar, M. Vazdar, Vibrational spectroscopy combined with molecular dynamics simulations as a tool for studying behavior of reactive aldehydes inserted in phospholipid bilayers, Chem. Phys. Lipids. 225 (2019) 104793. doi:10.1016/j.chemphyslip.2019.104793.

[29] R.N. Lewis, R.N.A.H.; Mannock, D.A.; McElhaney, Differential Scanning Calorimetry in the Study of Lipid Phase Transitions in Model and Biological Membranes, in: A.M. Dopico (Ed.), Methods Membr. Lipids, Humana Press, 2007: pp. 171–195.

[30] R.N.A.H. Lewis, R.N. McElhaney, Membrane lipid phase transitions and phase organization studied by Fourier transform infrared spectroscopy, Biochim. Biophys. Acta - Biomembr. 1828 (2013) 2347–2358. doi:10.1016/j.bbamem.2012.10.018.

[31] S. Šegota, D. Vojta, G. Pletikapić, G. Baranović, Ionic strength and composition govern the elasticity of biological membranes. A study of model DMPC bilayers by force- and transmission IR spectroscopy, Chem. Phys. Lipids. 186 (2015) 17–29. doi:10.1016/j.chemphyslip.2014.11.001.

[32] L.W. Hantao, H.G. Aleme, M.P. Pedroso, G.P. Sabin, R.J. Poppi, F. Augusto, Multivariate curve resolution combined with gas chromatography to enhance analytical separation in complex samples: A review, Anal. Chim. Acta. 731 (2012) 11–23. doi:10.1016/j.aca.2012.04.003.

[33] A. De Juan, J. Jaumot, R. Tauler, Multivariate Curve Resolution (MCR). Solving the mixture analysis problem, Anal. Methods. 6 (2014) 4964–4976. doi:10.1039/c4ay00571f.

[34] M. Maeder, A. de Juan, Two-Way Data Analysis: Evolving Factor Analysis, in: S. Brown, R. Tauler, B. Walczak (Eds.), Compr. Chemom., 2009: pp. 261–274. doi:10.1016/B978-044452701-1.00047-8.

[35] K. Cieślik-Boczula, B. Czarnik-Matusewicz, M. Perevozkina, M. Rospenk, MCR-ALS as an effective tool for monitoring subsequent phase transitions in pure and doped DPPC liposomes, RSC Adv. 5 (2015) 40455–40464. doi:10.1039/c5ra04234h.

[36] J. Jaumot, R. Gargallo, A. De Juan, R. Tauler, A graphical user-friendly interface for MCR-ALS: A new tool for multivariate curve resolution in MATLAB, Chemom. Intell. Lab. Syst. 76 (2005) 101–110. doi:10.1016/j.chemolab.2004.12.007.

[37] H.R. Keller, D.L. Massart, Evolving factor analysis, Chemom. Intell. Lab. Syst. 12 (1991) 209–224. doi:10.1016/0169-7439(92)80002-L.

[38] T.G. Mayerhöfer, J. Popp, Beyond Beer's Law: Revisiting the Lorentz-Lorenz Equation, ChemPhysChem. 21 (2020) 1218–1223. doi:10.1002/cphc.202000301.

[39] T.G. Mayerhöfer, J. Popp, Beer's Law – Why Absorbance Depends (Almost) Linearly on Concentration, ChemPhysChem. 20 (2019) 511–515. doi:10.1002/cphc.201801073.

[40] T.G. Mayerhöfer, A. Dabrowska, A. Schwaighofer, B. Lendl, J. Popp, Beyond Beer's Law: Why the Index of Refraction Depends (Almost) Linearly on Concentration, ChemPhysChem. 21 (2020) 707–711. doi:10.1002/cphc.202000018.

[41] B. Yoon, S.H. Kim, I. Lee, S.K. Kim, M. Cho, H. Kim, Dynamics of nematic MBBA film induced by transient grating under a strong absorption condition, J. Phys. Chem. B. 102 (1998) 7705–7713. doi:10.1021/jp981276k.

[42] T. Sato, K. Katayama, Direct measurement of the propagation of the phase-transition region of liquid crystals, Sci. Rep. 7 (2017) 44801. doi:10.1038/srep44801.

[43] G.W.H. Höhne, H.K. Cammenga, W. Eysel, E. Gmelin, W. Hemminger, The temperature calibration of scanning calorimeters, Thermochim. Acta. 160 (1990) 1–12.

[44] M. Pasenkiewicz-Gierula, Y. Takaoka, H. Miyagawa, K. Kitamura, A. Kusumi, Hydrogen Bonding of Water to Phosphatidylcholine in the Membrane as Studied by a Molecular Dynamics Simulation: Location, Geometry, and Lipid-Lipid Bridging via Hydrogen-Bonded Water, J. Phys. Chem. A. 101 (1997) 3677–3691. doi:10.1021/jp962099v.

[45] M. Pasenkiewicz-Gierula, Y. Takaoka, H. Miyagawa, K. Kitamura, A. Kusumi, Charge Pairing of Headgroups in Phosphatidylcholine Membranes: A Molecular Dynamics Simulation Study, Biophys. J. 76 (1999) 1228–1240. doi:10.1016/S0006-3495(99)77286-3.

[46] D.A. Pink, S. McNeil, B. Quinn, M.J. Zuckermann, A model of hydrogen bond formation in phosphatidylethanolamine bilayers., Biochim. Biophys. Acta. 1368 (1998) 289–305. doi:10.1016/S0005-2736(97)00196-X.

[47] F. Zhou, K. Schulten, Molecular Dynamics Study of a Membrane−Water Interface, J Phys Chem. 99 (1995) 2194–2207.

[48] M. Ge, J.H. Freed, Hydration, Structure, and Molecular Interactions in the Headgroup Region of Dioleoylphosphatidylcholine Bilayers: An Electron Spin Resonance Study, Biophys. J. 85 (2003) 4023–4040. doi:10.1016/S0006-3495(03)74816-4.

[49] G. Pabst, M. Rappolt, H. Amenitsch, P. Laggner, Structural information from multilamellar liposomes at full hydration: Full q-range fitting with high quality X-ray

data, Phys. Rev. E - Stat. Physics, Plasmas, Fluids, Relat. Interdiscip. Top. 62 (2000) 4000–4009. doi:10.1103/PhysRevE.62.4000.

[50] G. Cevc, Polymorphism of the bilayer membranes in the ordered phase and the molecular origin of the lipid pretransition and rippled lamellae, Biochim. Biophys. Acta. 1062 (1991) 59–69.